# Voxel-based T2 Relaxometry in Prion Disease

**E. De Vita[1,2], H. Hyare[3,4], C. Carswell[3,4], A. Thompson[3,4], A. Lukic[3,4], T. Yousry[1,2], P. Rudge [3,4], S. Mead[3,4], J. Collinge[3,4], and J. Thornton[1,2]**

[1]Lysholm Department of Neuroradiology, National Hospital for Neurology and Neurosurgery, UCLH NHS Foundation Trust, London, United Kingdom, [2]Academic Neuroradiological Unit, Department of Brain Repair and Rehabilitation, UCL Institute of Neurology, London, United Kingdom, [3]MRC Prion Unit, Department of Neurodegenerative Diseases, UCL Institute of Neurology, London, United Kingdom, [4]National Prion Clinic, National Hospital for Neurology and Neurosurgery, UCLH NHS Foundation Trust, London, United Kingdom

**Introduction.** Voxel-based analyses of cerebral T2 relaxometry data (VBR) [1] as originally applied in temporal lobe epilepsy [2], have recently found further applications in diseases including multiple system atrophy [3], amyotrophic lateral sclerosis [4] and studies of aging [5]. Human prion diseases are progressive neurodegenerative disorders caused by accumulation of aggregates of an abnormally folded prion protein, and provide a molecular model for neurodegeneration [6]. MRI methods sensitive to cerebral prion disease pathology include diffusion weighted imaging (DWI) [7] and magnetisation transfer ratio (MTR) measurement [8]. Here, quantitative cerebral T2 relaxometry is applied for the first time in prion disease patients; VBR is used to assess group differences between healthy controls (Ctr), subjects with symptomatic (IPD) and asymptomatic (As) inherited prion disease, and sporadic Creutzfeldt-Jacobs disease (sCJD). Voxel based morphometry (VBM) [9] results are shown for comparison.

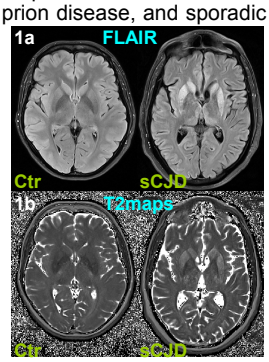


**Methods.** ***Subjects and MRI.*** We examined 69 subjects (24 Ctr, 19 As, 17 IPD, 9 sCJD) after informed consent at 3T (Siemens Tim TRIO) with a 32-channel head array coil. T2 relaxometry was performed with a turbo spin echo (TSE) sequence: TR 7s, TE1 27ms, TE2 108ms, echo train length 4, field of view (FoV) 256x192 $mm^2$, matrix 256x192, 55 contiguous 2.5mm axial slices, GRAPPA acceleration factor 2, total acquisition time (AT) 3'16". Also acquired were a 3D T1-weighted scan (MPRAGE, TR 2.2s, TE 2.9ms TI 900ms, echo spacing 6.7ms, flip angle 10º, FoV $(282mm)^2$, matrix $256^2$, 208 1.1mm sagittal partitions, AT 9'23"), standard clinical FLAIR-TSE (Fig 1a) and DWI. We excluded 14 subjects due to excessive motion in the T1 data; we thus analysed a total of 21 Ctr (median age/range 48/23-75 years), 19 As (44/21-57 years), 17 IPD (48/26-60 years), and 7 sCJD (59/53-70 years); 7 of these 62 (5 IPD, 2 sCJD) were excluded from the VBR analysis due to T2-acquisition motion artefacts.

***Data Processing and Analysis.*** FLAIR, TSE, T1 and DWI data were evaluated for signal intensity abnormalities by a neuro-radiologist. T2 maps were calculated according to: $T2 = (TE2-TE1) * ln (S_{TE2}/S_{TE1})$ (Fig 1b). VBR and VBM were performed with SPM8 [10] using 'unified segmentation' [11], and DARTEL [12] to generate cohort-specific grey and white matter (GM, WM) templates at $(1.5mm)^3$ resolution. Individual subject GM and WM segments were warped to these templates and smoothed (6mm Gaussian kernel). The 'optimal threshold' method [13] was used to generate GM and WM mask for statistical analysis. For VBR, the T2 maps were rigidly coregistered to the T1 data (with parameters computed on TE1 data), warped to the VBM template and smoothed (6mm kernel); the mask for VBR combined GM and WM VBM masks. Age and total intracranial volume (GM+WM plus cerebrospinal fluid (CSF) segments) were used as covariates. Group differences were evaluated with pairwise T-contrasts and family wise error (FWE) or false discovery rate (FDR) used to correct for multiple comparisons.

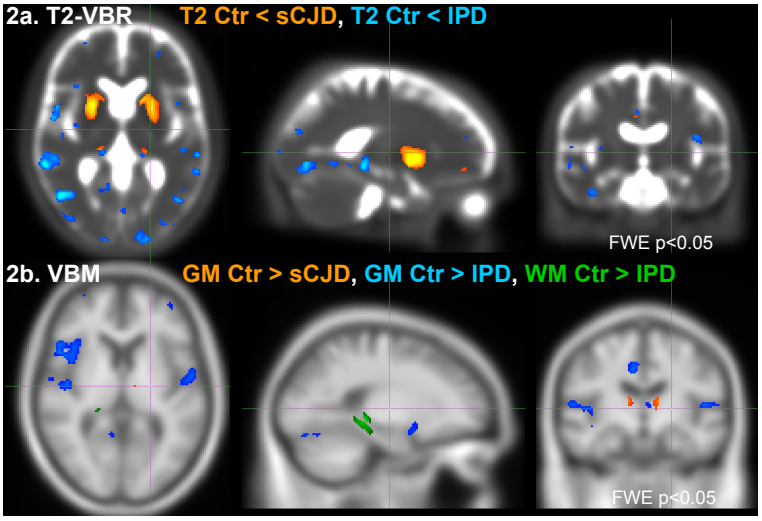


**Results.** Significant differences are shown for Ctr<sCJD and Ctr<IPD (T2-VBR), Ctr>sCJD and Ctr>IPD (GM-VBM) and Ctr>IPD (WM-VBM) for FWE p<0.05 (t-thresholds: 5.4 (T2), 5.2 (GM), 4.9(WM)) in fig. 2, on selected sections of the smoothed average T2 map or T1 image.

***As:*** There were no significant results for As *vs.* Ctr for both VBM and VBR, even with the much less stringent threshold: FDR p<0.05. As *vs* IPD and As *vs* sCJD contrasts showed similar (though less spatially extended) results as Ctr *vs* IPD and Ctr *vs* sCJD (see below)

***sCJD:*** Clusters of significantly increased T2 (*vs* Ctr) were apparent bilaterally in putamen, thalamus (LGN) and anterior limb of the internal capsule as well as in numerous cortical areas: anterior cingulate, rectal gyrus, Heschl gyrus (left only, L), superior temporal gyrus (right, R), middle frontal gyrus, middle cingulate cortex, fusiform gyrus. In VBM, no WM differences were seen even at FDR p<0.05. GM atrophy was only seen in the ventrolateral nucleus of thalamus (even for FDR p<0.05). For sCJD > IPD only the globus pallidus showed significant T2 increases. T2 values in the putamen (L, R average) were 74±3 ms (Ctr), 73±3 ms (As), 71±4 ms (IPD), 95±4 ms (sCJD), Of the 5 sCJD subjects included in the VBR analysis, abnormal signal was reported in cortex (n=3), basal ganglia (n=4) and thalamus (n=3) (Fig 1a).

***IPD:*** Numerous clusters of significantly increased T2 (*vs* Ctr) are apparent, with no overlap with sCJD results. However, in contrast to the sCJD results, most of these differences appear to be centred where the average T2 map shows CSF spaces (identifiable by extremely high T2 values). WM showed significant atrophy (*vs* Ctr) in the cortico-spinal tract (R), anterior-temporal WM (end of Meyers loop)(L), hippocampus, inferior and superior frontal gyri (R); only the hippocampal area overlapped with significant T2 increases. GM showed significant atrophy (*vs* Ctr) in the parahippocampal gyrus, mid-orbital gyrus, superior temporal gyrus, insular cortex, middle cingulate, supramarginal gyrus (L), post-central gyrus (L).

**Discussion.** On VBR analysis the most robust T2 increases *vs* healthy Ctr were seen for the sCJD group, all in areas were VBM detected no atrophy. Although most of these areas were apparent by visual assessment on conventional imaging, T2 relaxometry provides objective, quantitative indices that are likely to reflect the underlying pathology and could be used to follow the clinical progression of sCJD, and potentially to monitor the effects of therapy. For the IPD patients, the results provided by T2-VBR are less easily interpreted. Inspection of the individual datasets suggests that most areas of significant difference are associated with widening of the CSF spaces in the IPD group; T2 measurements over some of these clusters support the suggestion that they are likely reflect CSF contamination rather than true parenchymal T2 changes. However it is of note that no significant atrophy was detected by VBM in most of these regions. Future work will address this issue: it may be possible to refine our VBR analysis by masking out voxels with substantial CSF contamination and performing the smoothing step in an anisotropic fashion [2]; at the same time these potentially CSF-associated artefactual T2 changes may prove more sensitive in detecting brain tissue loss than conventional VBM.

**Conclusions.** T2-VBR identified areas of pathological change distinct to those indicated by VBM and highlighted differences between the subtypes of prion disease; voxel based T2 relaxometry provides, with an additional acquisition time of little more than 3 minutes, a sensitive measure of cerebral prion pathology and offers potentially distinct but complementary information to that available from VBM, DWI and MTR.

***References.*** *[1] Pell GS, Neuroimage **21**:707, 2004 [2] Pell GS, Neuroimage **39**:1151, 2008 [3] Tzarouchi LC, J Neuroimaging **20**:260, 2010 [4] Minnerop M, J Neurol **256**:28, 2009 [5] Hasan KM, Magn Reson Med. **64**:1382, 2010 [6] Ross C, Nature Medicine **10**:S10, 2004 [7] Hyare H, Neurology **74**:658, 2010 [8] Siddique D, Brain **10**:3058, 2010 [9] Ashburner J, Neuroimage **11**:805, 2000 [10] http://www.fil.ion.ucl.ac.uk/spm/software/spm8 [11] Ashburner J, Neuroimage **26**:839, 2005 [12] Ashburner J, Neuroimage **38**:95, 2007 [13] Ridgway G, Neuroimage **44**:99, 2009.*